

Ground state of the U_2Mo compound: Physical properties of the Ω -phase



E.L. Losada ^a, J.E. Garcés ^{b,*}

^a SIM3, Centro Atómico Bariloche, Comisión Nacional de Energía Atómica, Argentina

^b GIA, Centro Atómico Bariloche, Comisión Nacional de Energía Atómica, Argentina

ARTICLE INFO

Article history:

Received 9 March 2016

Received in revised form

14 June 2016

Accepted 23 June 2016

Available online 27 June 2016

ABSTRACT

Using *ab initio* calculations, unexpected structural instability was recently found in the ground state of the U_2Mo compound. Instead of the unstable $I4/mmm$ and the $Pmmm$ structures, in this work the $P6/mmm$ (#191) space group, usually called Ω -phase, is proposed as the fundamental state. Total energy calculations using Wien2k code slightly favoured the last structure. Electronic and elastic properties are studied in this work in order to characterize the physical properties of this new phase. The stability of the Ω -phase is studied by means of its elastic constants calculation and phonon dispersion spectrum. Analysis of isotropic indices shows that the new phase is a ductile material with a minimal degree of anisotropy, suggesting that U_2Mo in the $P6/mmm$ structure is an elastic isotropic material. Analysis of charge density, density of electronic states (DOS) and the character of the bands revealed a high level of hybridization between *d*-molybdenum electronic states and *d*- and *f*-uranium ones.

© 2016 Elsevier B.V. All rights reserved.

1. Introduction

Renewed interest has recently been shown in the U-Mo system. The main reasons are related to its relevance as a potential nuclear fuel to be used in Material Testing Reactor (MTR) [1] and *GenIV* power reactors [2]. However, it is also due to the unusual physical properties found in the ground state of this system [3]. The unique stable compound observed in the phase diagram at finite temperature is U_2Mo . The ground state of this compound was previously assumed to be the C11b structure (MoSi2 prototype, $I4/mmm$ space group), since there was no information to contradict this hypothesis. Detailed theoretical calculations also found one compound in the ground state of the U-Mo system [4,5]. Nevertheless, it was shown in Refs. [6,7] that the assumed C11b structure is unstable under the D_6 deformation associated with the C_{66} elastic constant. It was proposed in Ref. [6], using the USPEX code, that the ground state of the U_2Mo compound has the $Pmmm$ structure.

The same result regarding the above-mentioned instability was obtained in Ref. [3] through analysis of the elastic constants. In

addition, those results showed that the structure of the ground state of the U_2Mo compound could be other than the assumed C11b and the $Pmmm$ structures. Taking into account more isotropic atomic arrangements and computing the total energy using the WIEN2k code [8], a more symmetric structure was found, which is energetically more stable than the $Pmmm$ one. The $P6$ space group (#168) was proposed as the ground state of the U_2Mo compound, as it is $\sim 0.1mRy$ more stable than the $Pmmm$ structure, the total energy of both structures being computed in the primitive unit cell. The root causes of the structural instability were also explained in Ref. [3]. It was found that the distorted structure is stabilized due to the split of the *f*-band of U and the relocation below the Fermi level (FL) of the hybridized states between Mo and U atoms. The characteristic distance between parallel chains, composed by consecutive U-Mo-U blocks in the $I4/mmm$ (2.435 Å), changes to two distances (2.3627 Å and 2.509 Å) in the stable $P6/mmm$ structure ($\delta = \pm 0.03$). These changes modify the U-U interaction and reproduce the same situation as that observed in Ref. $\alpha-U$ where a Peierls distortion is found. Söderlind et al. [9] showed that the crystal structure in pure uranium is determined by the balance between Madelung interactions and a Peierls distortion of the lattice, which favour low symmetry structures. However, whereas the Peierls distortion in $\alpha-U$ is spontaneous, in U_2Mo it is induced by

* Corresponding author.

E-mail address: garcés@cab.cnea.gov.ar (J.E. Garcés).

the deformation D_6 .

Instead of the unstable $I4/mmm$ structure and the recently proposed $Pmmn$ one, it is suggested in this work that the ground state has the $P6/mmm$ (# 191) space group symmetry, usually called Ω -phase, as it is shown in Fig. 1. This work presents a detailed *ab initio* study of the physical properties of this novel structure in the U-Mo system, providing useful information applicable to modelling phase diagrams of multicomponent nuclear fuels. The stability of the Ω -phase is analysed using the Phonon package and computing of the elastic constants and modules. The total energies for these calculations are obtained from the Wien2k code. The electronic properties are computed in order to explain the elastic isotropic behaviour of the new ground state structure.

This paper is organized as follows. Section 2 describes the theoretical methodology. The results and discussion are presented in Section 3: i) Subsection 3.1 shows the ground state structural properties, ii) Subsection 3.2 discusses the elastic and phonon properties, and iii) Subsection 3.3 summarizes the electronic structure and nature of chemical bonds in the Ω -phase structure. The conclusions are presented in Section 4.

2. Theoretical methodology

The total energy of U_2 Mo in all structures, i.e. $C11b$, $Pmmn$ and $P6/mmm$, were computed using the full potential LAPW method based on the density functional theory as implemented in the WIEN2k code. This code uses the full-potential LAPW + lo method that makes no shape approximation to the potential or density. Electronic exchange-correlation interactions were treated within the generalized gradient approximation of Perdew, Burke and Ernzerhof [10], as no experimental or theoretical evidence of strong correlations was found in the system studied here. The radii of the atomic spheres (RMT) selected for U and Mo were $R_{MT} = 2.3a.u.$ and $R_{MT} = 1.8a.u.$, respectively. In order to describe the electronic structure of all the atoms and their orbitals, the APW + lo basis set was selected. Local orbital extensions were included to describe the semicore states. The cut-off parameter that controls convergence in the expansion of the solution to the Kohn-Sham equations was chosen to be $Rk_{max} = 8$, where k_{max} is the plane wave cut-off and R_{MT} is the smallest of all the atomic sphere radii. The maximum l values for partial waves used inside the atomic spheres and for the non-muffin-tin matrix elements were selected to be $l_{max} = 10$ and $l_{max} = 4$, respectively. The charge density cut-off G_{max} was selected as $22Ry^{1/2}$. A mesh of 50000 k -points was used in the whole Brillouin zone to study the electronic properties of the fundamental state. k -space integration was calculated using the modified tetrahedron-method [11]. The iteration process was repeated until

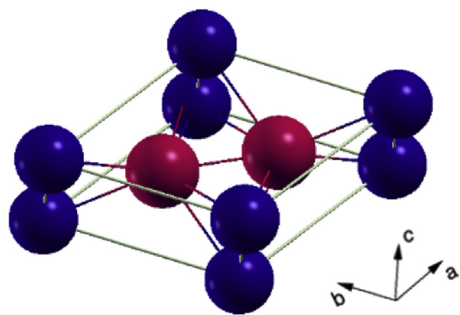


Fig. 1. Ω -phase ground state structure of the U_2 Mo compound. Space group $P6/mmm$ (#191). $a = b = 4.8207$ Å and $c = 2.7643$ Å. Blue: Mo atoms. Red: U atoms. (For interpretation of the references to colour in this figure legend, the reader is referred to the web version of this article.)

the calculated total energy converged to less than 1×10^{-6} Ry/cell, and the calculated total charge converged to less than 1×10^{-6} e/cell. In order to calculate the internal parameters of the crystal structures, we employed the mini LAPW script implemented in the Wien2K package. The calculations were performed without including spin-orbit interactions, since no significant effects were observed near the Fermi level, as previously shown in Ref. [3].

The phonon band structure and thermal properties of the U_2 Mo Ω -phase were calculated using the finite displacement method implemented in the Phonopy [12] package. This method involves the creation of a supercell and introduction of atomic displacements. The 24-atom supercell was composed of $2 \times 2 \times 2$ primitive unit cells. The forces acting on atoms of the supercells were calculated with the Wien2k code with a precision of 0.1 mRy/a.u. The phonopy post-process uses these forces to calculate phonon related properties: phonon band structure, total and partial density of states, and thermal properties.

3. Results and discussion

3.1. Ground state of the U_2 Mo compound

The instability observed in the $C11b$ structure [3,6,7] reveals that the ground state of U_2 Mo compound has a different crystalline structure. Wang et al., using the USPEX code, suggested the $Pmmn$ structure as the new ground state. The difference in energy between the $I4/mmm$ and $Pmmn$ structures, using the Wien2k code, is ~ 5 mRy per primitive unit cell. Both structures are characterized by different U-Mo distances. Whereas the distance is 3.1147 Å in the $I4/mmm$ structure, the $Pmmn$ computed using the Wien2k code ($a = 4.8251$ Å, $b = 8.3504$ Å, $c = 2.7726$ Å) has two characteristic distances, one at 3.1083 Å and the other at 3.1118 Å. Although the structure proposed by Wang et al. overcomes the instability, the slightly different U-Mo distances within the structure rises the question of whether another structure could be more stable than the $Pmmn$. A search was performed in the belief that the structure at 0° K should have more symmetries than the $Pmmn$ one. The XCrySDen [13] code was used to analyse the symmetry of probable candidates, using the $Pmmn$ structure as the starting point, and computing total energy with the WIEN2k code. A hexagonal structure was found to be marginally more stable than the $Pmmn$ one. It was suggested in our previous work that the structure with the $P6$ space group (# 168) could be another alternative for the ground state of the U_2 Mo compound, as it is a more symmetric structure. The total energy difference between both structures in the GGA approximation is ~ 0.1 mRy per primitive unit cell. In any case, only experiments will validate any of them or find the actual ground state structure.

The $P6$ space group was used to obtain freedom in the atomic movements in order to optimize the $Pmmn$ structure. However, if all symmetries are included the actual space group is the $P6/mmm$ (# 191). This structure has the AlB_2 prototype usually known as Ω -phase [14]. The structure is formed alternating close-packed hexagonal layered structures of Mo and graphite-like U layers. The lattice parameters of the structure are $a = b = 4.8207$ Å and $c = 2.7643$ Å. It has one Mo atom at Wyckoff position 1(a): (0,0,0) and two U atoms at positions 2(b): ($1/3, 2/3, z$) and ($2/3, 1/3, z$); where $z = 0.5$. The Mo atoms have 12 U neighbours at a distance of 3.1075 Å. Each U atom is surrounded by 5 U atoms. Three of these are coplanar at a distance of 2.7832 Å and two lie along the c axis, at a distance of 2.7643 Å. The c lattice parameter used in a previous study [3] ($c = 2.7726$ Å) was adjusted to the value presented in this work. The difference in lattice parameter is due to a more accurate total energy vs. D_3 distortion calculation.

The structures $I4/mmm$, $Fmmm$, $Pmmn$ and $P6/mmm$ have one

feature in common which is the existence of U-Mo-U blocks. Indeed, the first two structures can be interpreted as being formed by parallel linear chains along the z-directions, each one composed of consecutive U-Mo-U blocks. We found that in the $P6/mmm$ ground state structure the chains characterizing the $I4/mmm$ structure were broken and two consecutive blocks were displaced mainly perpendicular to the chains. The new structure overcame the instability by this mechanism.

3.2. Structural stability of the U_2 Mo Ω -phase

3.2.1. Elastic properties

Elastic constants describe the behaviour of crystals as a function of elastic deformations. Elastic properties are related to mechanical and thermal properties such as specific heat, thermal expansion, Debye temperature, melting point, and Grüneisen parameter. They also give information about the anisotropic character of bonding in crystals.

Elastic constants are obtained by computing the second order derivatives of the total energy with respect to the distortion parameter. This calculation is very sensitive to data point selection, due to numerical inaccuracies around the minimum of total energy vs. atomic displacements. There are only five independent elastic constants for hexagonal crystals Ref. [15]. They can be determined by imposing strains, either individually or in combination, along specific crystallographic directions. The elastic constants used in this work are C_{11} , C_{12} , C_{13} , C_{33} , C_{55} , and the symmetry relationship with the remaining ones are:

$$C_{11} = C_{22} \quad (1)$$

$$C_{13} = C_{23} \quad (2)$$

$$C_{55} = C_{44} \quad (3)$$

$$C_{66} = \frac{1}{2}(C_{11} - C_{12}) \quad (4)$$

$$C_{ZZ} = 2C_{11} + 2C_{12} + 4C_{13} + C_{33} \quad (5)$$

The distortion matrices described by Fast et al. [16], are used in this work to compute the elastic constants for this structure. Table 1 summarizes the information regarding space group, distortion matrices and the third-order polynomial fitting to Wien2k results. The three distortions involving $(C_{11} + C_{22})$, C_{33} and C_{44} do not change the hexagonal symmetry ($P6/mmm$) but $(C_{11} - C_{12})$ and C_{ZZ} do change the symmetry from hexagonal to orthorhombic and monoclinic, respectively. The positions of non-equivalent Mo and U atoms in the hexagonal $P6/mmm$ space group are fixed in special positions, and consequently, relaxation of internal coordinates is not necessary. The Mo atom positions remain fixed by symmetry to the corner positions of the crystal cell for distortions $C_{11} - C_{12}$ and C_{ZZ} , but the position of U atoms should be fully relaxed in order to compute these elastic constants. The relaxation procedure, as implemented in the code Wien2k, was stopped for interatomic forces lower than $2mRy/a.u.$ Table 2 compares the results of this work for the $P6/mmm$ structure with the $Pmmn$ one [6].

The energy associated with the five distortions and the elastic constants deduced from them are summarized below. In the following equations, V_0 is the volume of the unstrained system, $E(V_0, \delta)$ is the total energy computed by the *ab initio* code, and τ_1 , τ_2 , τ_3 and τ_5 are the elements of the stress tensor in Voigt notation ($\tau_1 = \tau_{xx}$, $\tau_2 = \tau_{yy}$, $\tau_3 = \tau_{zz}$ and $\tau_5 = \tau_{xz}$).

$$E(V, \delta) = E(V_0, 0) + V_0 [(\tau_1 + \tau_2)\delta + (C_{11} + C_{12})\delta^2] \quad (6)$$

$$C_{11} + C_{12} = \frac{1}{2V_0} \frac{d^2(E - E_0)}{d\delta^2} \quad (7)$$

$$E(V, \delta) = E(V_0, 0) + V_0 [(\tau_1 - \tau_2)\delta + (C_{11} - C_{12})\delta^2] \quad (8)$$

$$C_{11} - C_{12} = \frac{1}{2V_0} \frac{d^2(E - E_0)}{d\delta^2} \quad (9)$$

$$E(V, \delta) = E(V_0, 0) + V_0 \left[\tau_3 \delta + \frac{C_{33}}{2} \delta^2 \right] \quad (10)$$

$$C_{33} = \frac{1}{V_0} \frac{d^2(E - E_0)}{d\delta^2} \quad (11)$$

$$E(V, \delta) = E(V_0, 0) + V_0 [\tau_5 \delta + 2C_{55} \delta^2] \quad (12)$$

$$C_{55} = \frac{1}{4V_0} \frac{d^2(E - E_0)}{d\delta^2} \quad (13)$$

$$E(V, \delta) = E(V_0, 0) + V_0 \left[(\tau_1 + \tau_2 + \tau_3)\delta + \frac{1}{2}C_{ZZ}\delta^2 \right] \quad (14)$$

$$C_{ZZ} = \frac{1}{V_0} \frac{d^2(E - E_0)}{d\delta^2} \quad (15)$$

The deformation energy ($\frac{1}{2}C_{ij}e_i e_j$) must be positive definite to ensure the mechanical stability of the crystal. This implies further restrictions on the C_{ij} found by algebraical methods. For a crystal with hexagonal symmetry, the constraints [15] are:

$$C_{44} > 0, C_{11} > |C_{12}|, (C_{11} + C_{12})C_{33} > 2C_{13}^2 \quad (16)$$

U_2 Mo in the $P6/mmm$ structure is mechanically stable, since all its elastic constants fulfil the above requirements. The elastic constants C_{11} and C_{33} have the largest values and represent the elasticity along directions parallel and perpendicular to the basal plane; x- and z- directions respectively. The result can be interpreted as showing that the bonding characters along the x- and z-directions are the two strongest of all the directions. The other three elastic constants, C_{12} , C_{13} and C_{44} , are related to the elasticity of shape deformation. Therefore, their similar values show that the crystal presents almost the same response to this kind of deformation.

Based on the calculated elastic constants, the theoretical polycrystalline bulk modulus B and shear modulus G can be determined from their sets of elastic constants using the approximations of Voigt [17], Reuss [18] and Hill [19]. While the Voigt approach gives the upper bound of elastic properties, the Reuss approach provides the lower bound. For the Voigt average, the bulk and shear moduli for hexagonal systems are given by:

$$B_V = \frac{1}{9} [2(C_{11} + C_{12}) + C_{33} + 4C_{13}] \quad (17)$$

$$G_V = \frac{1}{30} (M + 12C_{44} + 12C_{66}) \quad (18)$$

For the Reuss average [18], the moduli are given by,

Table 1
Distortion matrices, space group, Wien2k results and third order polynomial fit used to compute the five elastic constants of the $P6/mmm$ ground state. C_{ZZ} stands for the following elastic constants combination: $C_{ZZ} = 2C_{11} + 2C_{12} + 4C_{13} + C_{33}$.

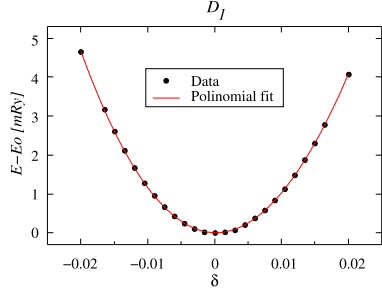
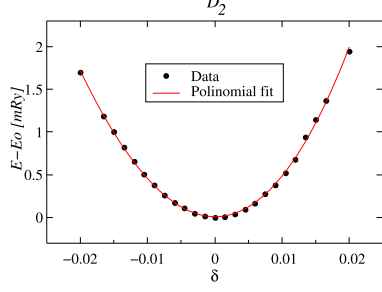
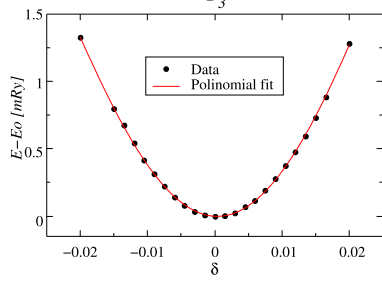
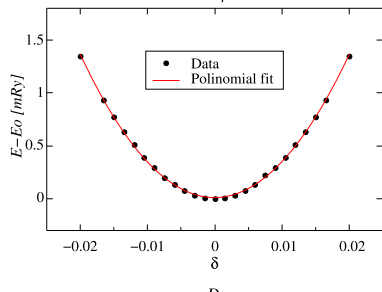
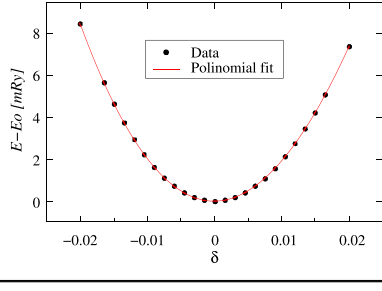
Combination of elastic constants	Deformation matrix	Space group	Polynomial fit
$C_{11} + C_{12}$	$D_1 = \begin{pmatrix} 1+\delta & 0 & 0 \\ 0 & 1+\delta & 0 \\ 0 & 0 & 1 \end{pmatrix}$	$P6/mmm(\#191)$	
$C_{11} - C_{12}$	$D_2 = \begin{pmatrix} 1+\delta & 0 & 0 \\ 0 & 1-\delta & 0 \\ 0 & 0 & 1 \end{pmatrix}$	$Cmmm(\#65)$	
C_{33}	$D_3 = \begin{pmatrix} 1 & 0 & 0 \\ 0 & 1 & 0 \\ 0 & 0 & 1+\delta \end{pmatrix}$	$P6/mmm(\#191)$	
C_{55}	$D_4 = \begin{pmatrix} 1 & 0 & \delta \\ 0 & 1 & 0 \\ \delta & 0 & 1 \end{pmatrix}$	$C2/m(\#12)$	
C_{ZZ}	$D_5 = \begin{pmatrix} 1+\delta & 0 & 0 \\ 0 & 1+\delta & 0 \\ 0 & 0 & 1+\delta \end{pmatrix}$	$P6/mmm(\#191)$	

Table 2

Comparison between the elastic constants calculated in this work for the $P6/mmm$ structure and the $Pmmn$ one proposed by Wang et al. (* stands for constants obtained by symmetry operations.).

Space group	C_{11}	C_{12}	C_{13}	C_{22}	C_{23}	C_{33}	C_{44}	C_{66}	Reference
$P6/mmm$	304	123	103	304*	103*	288	66	90*	This work.
$Pmmn$	299	131	116	293	17	246	74	87	Wang et al. [6]

$$B_R = \frac{C^2}{M} \quad (19)$$

$$G_R = \frac{5}{2} \frac{C^2 C_{44} C_{66}}{3 B_V C_{44} C_{66} + C^2 (C_{44} + C_{66})} \quad (20)$$

$$M = C_{11} + C_{12} + 2C_{33} - 4C_{13} \quad (21)$$

$$C^2 = (C_{11} + C_{12})C_{33} - 2C_{13}^2 \quad (22)$$

Hill proved that the Voigt and Reuss methods resulted in the theoretical upper and lower bounds of the isotropic elastic modulus, respectively. Hill suggested a practical estimation of the bulk and shear moduli as the arithmetic means of both values. The bulk and shear moduli are computed in the Hill empirical average as,

$$B_H = (B_V + B_R)/2, \quad (23)$$

$$G_H = (G_V + G_R)/2. \quad (24)$$

From these values, Young's modulus E and Poisson's ratio ν can be computed as,

$$E = \frac{9B_H G_H}{3B_H + G_H} \quad (25)$$

$$\nu = \frac{3B_H - 2G_H}{2(3B_H + G_H)} \quad (26)$$

Based on the fact that the shear modulus G represents the resistance to plastic deformation while the bulk modulus represents resistance to fracture, Pugh [20] introduced the ratio between the bulk and shear moduli, B/G , for polycrystalline phases as a measure of the fracture/toughness of metals. A value greater than 1.75 is associated with ductility and a lower brittleness behaviour. This value for $U_2 Mo$ in the $P6/mmm$ structure is $B/G = 2.13$. This result indicates that $U_2 Mo$ has ductile behaviour. The ductility of this compound is confirmed by the values of Poisson's ratio, a property also used to measure the ductility and brittleness of materials [21]. The critical value which separates ductility from brittleness is 0.26 [22]. The value of $\nu = 0.3$, showed in Table 3, confirms the ductile character of the $U_2 Mo$ compound with the Ω -phase structure.

Analysis of elastic anisotropy allows understanding of the bonding nature of a crystal. It can be described either through the universal anisotropic index A^U proposed by Ranganathan and

Ostioja-Starzewski [23] for crystals with any symmetry defined by,

$$A^U = 5 \frac{G_V}{G_R} + \frac{B_V}{B_R} - 6 \geq 0, \quad (27)$$

or through the percent anisotropy indexes of bulk and shear moduli (A_B and A_G), proposed by Chung and Buessen [24,25], defined by,

$$A_B = \frac{B_V - B_R}{B_V + B_R}, \quad (28)$$

$$A_G = \frac{G_V - G_R}{G_V + G_R}. \quad (29)$$

The Voigt and Reuss approximations should give the same values for B and G modules for isotropic structures. Consequently, deviations from zero indicate anisotropy. The results for the anisotropic indexes are shown in Table 3. It can be seen that $A_U = 0.15$ and the percent anisotropy, both in shear $A_G = 0.014$ and compression $A_B = 0.0014$, are almost zero suggesting that $U_2 Mo$ in the $P6/mmm$ structure is an elastic isotropic material. The minimal degree of anisotropy and the values of elastic constants exhibited can be understood by examining the nature of chemical bonds between atoms.

3.2.2. Phonon dispersion relation

The dynamical stability of $U_2 Mo$ in the $P6/mmm$ structure requires the energies of phonons to be positive for all wave vectors in the Brillouin zone (BZ). The phonon dispersion relations are computed with the Phonopy code by constructing a $2 \times 2 \times 2$ supercell. The path in the reciprocal lattice along the high-symmetry points of the hexagonal BZ considered to calculate the phonon dispersion is $\Gamma-A-L-H-A-L-M-K-H-L$, and is depicted in Fig. 2. The full phonon dispersion of the $U_2 Mo$ compound consists of 9 branches: 3 acoustic and 6 optics. The results obtained are shown in Fig. 3. The phonon dispersion curves do not present imaginary frequencies, showing the dynamical stability of the Ω -phase of the $U_2 Mo$ compound, in agreement with the results obtained by analysing elastic constants. The phonon densities of state can be clearly separated by Mo and U due to the very different masses of U and Mo atoms. The low-frequency region (below 4THz)

Primitive Brillouin Zone

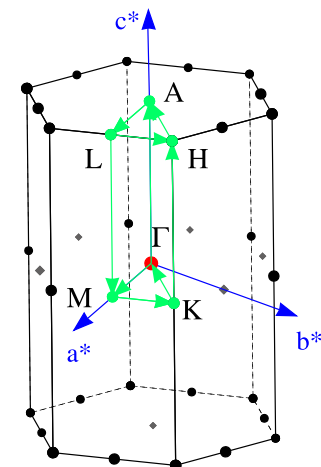


Fig. 2. Brillouin zone of hexagonal type lattice [26] with the selected path for phonon dispersion curves and band structure calculations.

Table 3

Elastic moduli and anisotropy indices for the Ω -phase of $U_2 Mo$ compound.

Space group	B	G	E	ν	B/G	A^U	A_B	A_G
$P6/mmm$	173	81	210	0.3	2.13	0.15	0.00139	0.0144

is dominated by the U atom because the acoustic modes originate mainly from heavy elements, and above 4THz the phonon modes are mainly from the Mo atoms, in agreement with previous results [6].

3.3. Electronic structure and nature of chemical bonds

The results of previous sections present the $P6/mmm$ structure of the $U_2 Mo$ compound as a ductile material with a minimum degree of anisotropy. The reasons behind these properties can be understood by examining the electronic properties and chemical bonding between the U and Mo atoms.

Figs. 4 and 5 show the charge density plots for planes with Miller-Bravais indices $(0\ 0\ 0\ 2)$ and $(1\ 1\ \bar{2}\ 0)$. The charge density is strongly directional and concentrated between U and Mo planes with chemical bonds of lower strength between U-U and Mo-Mo atoms. The charge density distribution between U atoms in the $(0\ 0\ 0\ 2)$ plane and along the c-axis are similar, as shown in Figs. 4 and 5. The result of the strong bond between U and Mo is such that the structure is characterized by one Mo atom surrounded by twelve U, each U being surrounded by six Mo atoms and five U atoms. The charge density plots reveal the main reason for the elastic isotropic behaviour of this structure: the U and Mo atoms have an almost chemically isotropic environment.

The strength of the interatomic bonds and elastic properties of materials are determined mainly by the occupied states at and near the Fermi level. Consequently, analysis of the DOS below the Fermi level will identify the electronic state responsible for the symmetric charge density distribution and the consequent elastic isotropic behaviour of $U_2 Mo$.

Figs. 6 and 7 show the total and projected DOS for the different electronic states of Mo and U, respectively. The main contributions to the DOS near the Fermi level are due to the d-orbitals of Molybdenum and the d- and f-orbitals of Uranium. The projected DOS show that the location of these orbitals could be hybridized, as they are located almost in the same energy range near the FL. The band character will be computed along the path showed in Fig. 2, in order to study this possibility. The remaining electronic states have negligible contributions near the FL. However, the s- and p-electronic states of both atoms make their main contribution between 4–5 eV below the FL.

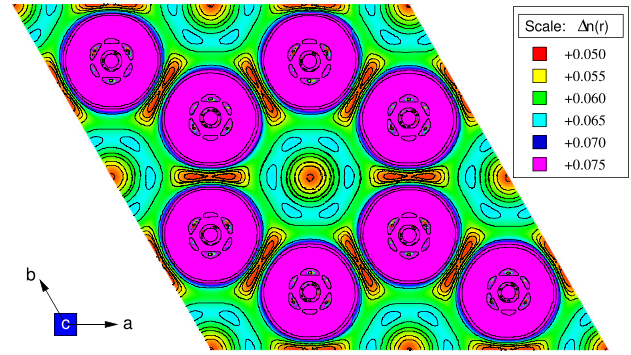


Fig. 4. Charge density distribution on the $(0\ 0\ 0\ 2)$ plane of the Ω -phase.

Fig. 8 shows the character of the bands for the relevant states near the FL. Whereas the only relevant orbital for Mo is the d-state, the main contribution for U comes from both the d- and f-states. Fig. 8 shows strong hybridization between f-U and d-Mo states along the line $\Gamma-M-K-\Gamma$, and also along the $A-L$, $L-M$ and $M-K$ lines. Hybridized states between d-Mo and d-U can be observed

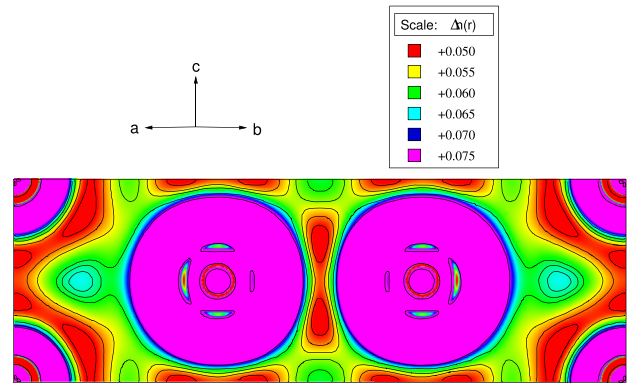


Fig. 5. Charge density distribution on the $(1\ 1\ \bar{2}\ 0)$ plane of the Ω -phase.

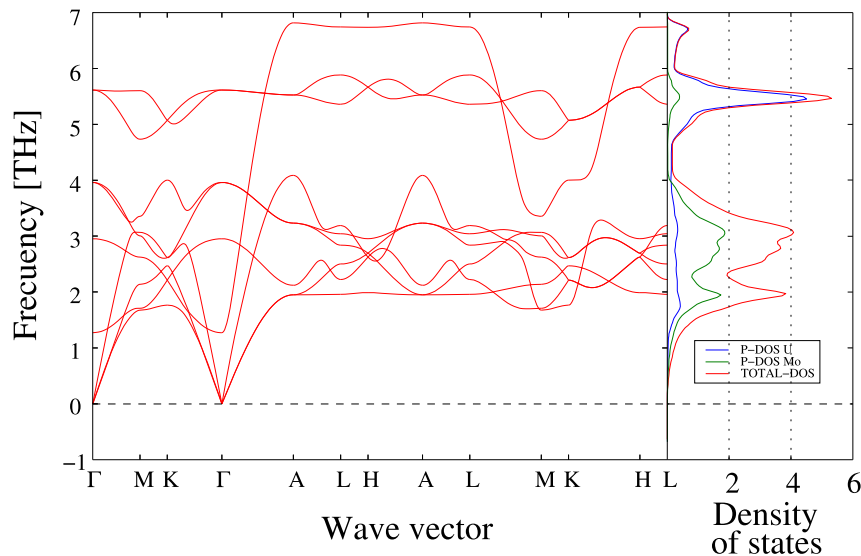


Fig. 3. Calculated phonon dispersion curves (left) and projected phonon density of states (right) of the $U_2 Mo$ Ω -phase.

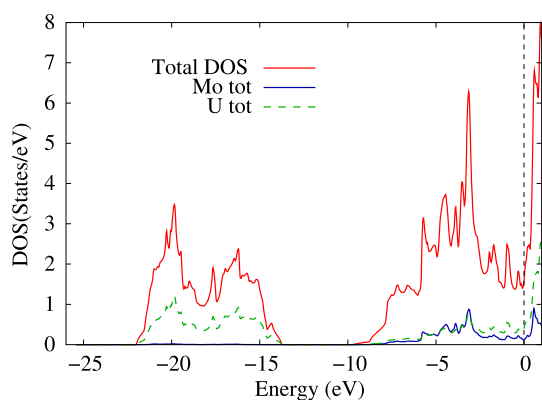


Fig. 6. Calculated total density of states (red line) and atom-projected densities inside muffin-tin spheres (Mo: blue line, U: green line) of electron states for the Ω -phase of the U_2 Mo compound. (For interpretation of the references to colour in this figure legend, the reader is referred to the web version of this article.)

mainly along the K – Γ direction.

In summary, the bands with character plot show significant hybridization between d-Mo and d- and f-U states. Although the ground state structure is characterized by strong bonding and almost isotropic U-Mo interactions, the $P6/mmm$ structure becomes unstable by increasing the temperature stabilizing the $I4/mmm$ one.

4. Conclusions

The U-Mo system has technological relevance as a potential fuel

in experimental reactors and in GenIV reactors. The unexpected physical behaviour found recently in the ground state reveals that the system is still not fully characterized. The available information suggests the $C11b$ ($MoSi_2$ prototype $I4/mmm$ space group) structure as the ground state of this compound. It was shown, however, in Refs. [3,6,7] that the assumed $C11b$ structure is unstable under the D_6 distortion associated with the C_{66} elastic constant. The root causes of this structural instability are related to the existence of a Peierls distortion induced by the deformation D_6 [3]. The results of this work show the $P6/mmm$ space group, usually called Ω -phase, to be the structure of the ground state. This work presents a detailed *ab initio* study of the U-Mo ground state, in order to identify its main physical properties. This information can be useful in modelling the U-Mo system and multicomponent phase diagram of nuclear fuels, mainly with theoretical tools based on ground state properties.

The stability of the Ω -phase is analysed by computing the elastic constants. All of these verify the stability criterion. Analysis of the isotropic indexes shows that the new structure is a ductile material which has a minimal degree of anisotropy, suggesting that U_2 Mo in the $P6/mmm$ structure is an elastic isotropic material. The phonon dispersion spectrum does not show imaginary frequencies, supporting the dynamic stability found by analysing the elastic constants. The phonon densities of state are clearly separated by Mo and U due to the very different masses of U and Mo atoms. The low-frequency region (below 4 THz) is dominated by the U atom because the acoustic modes originate mainly from heavy elements, while above 4 THz the phonon modes are mainly from the Mo atoms, in agreement with previous results [6]. The electronic properties such as DOS, charge density and character of bands reveal a high level of hybridization between the d-electronic states

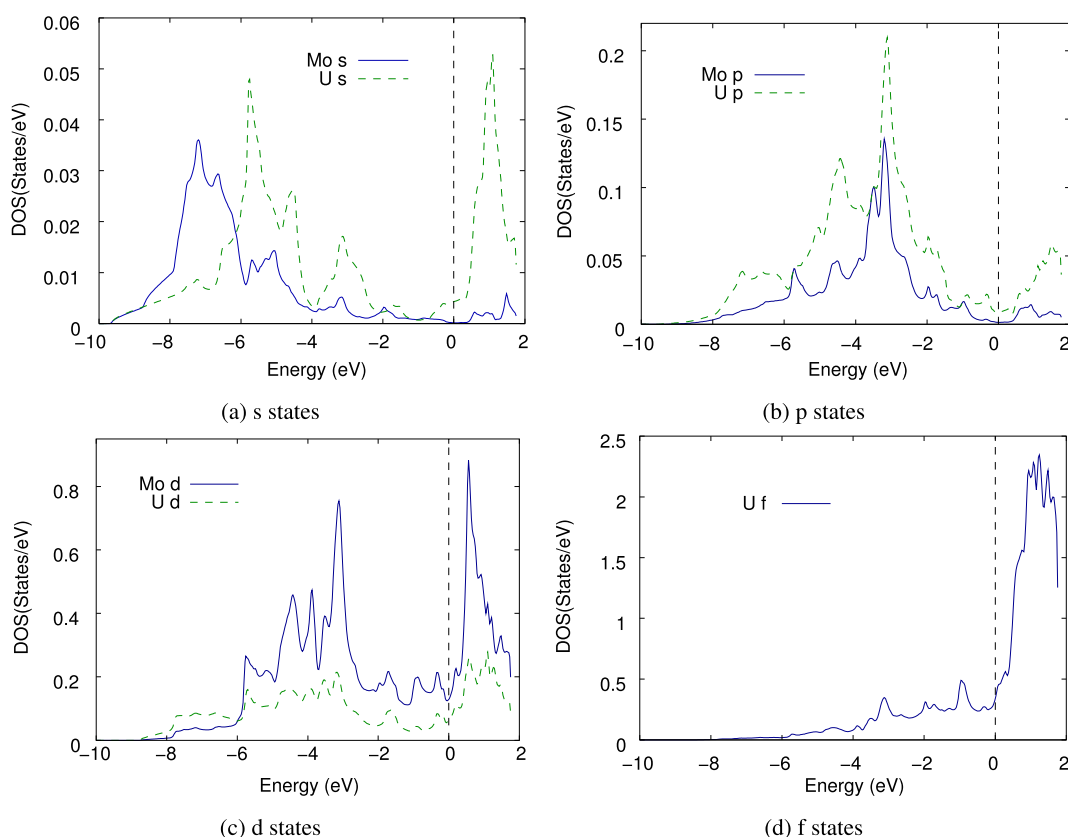


Fig. 7. Projected densities of states for Mo and U atoms in the range -10 eV to 2 eV: a) s-states, b) p-states, c) d states and d) f-states.

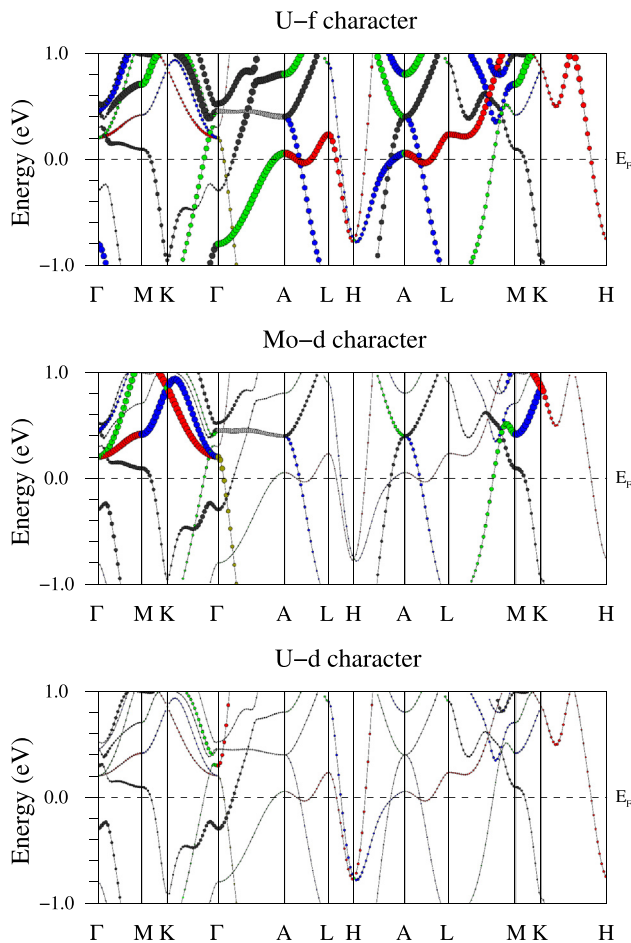


Fig. 8. Band character of the Ω -phase near the Fermi level obtained following the path depicted in Fig. 2. Number of k -points = 50000. a) f character of U, b) d character of Mo and c) d character of U.

of Molybdenum and the d- and f-states of Uranium atoms. The charge density is strongly directional and concentrated between U and Mo planes, with lower-strength chemical bonds between U-U and Mo-Mo atoms. The charge density plots reveal the main reason for the elastic isotropic behaviour of this structure, i.e. the U and Mo atoms have an almost chemically isotropic environment.

The unexpected instability of the C11b compound and the existence of a new ground state with the Ω -phase structure raises the question of whether other compounds with different compositions

and structures may exist in the ground state of the U-Mo system. Furthermore, detailed research is needed to fully characterize the ground state of this system and to understand the relationship between the ground state properties, the superconductivity of metastable phases [27,28] and the asymmetric shape of the heat of formation vs. Mo concentration for the disordered bcc solid solution [5].

References

- [1] J. Snelgrove, G. Hofman, M. Meyer, C. Trybus, T. Wiencek, Nucl. Eng. Des. 178 (1997) 119.
- [2] Y.S. Kim, G. Hofman, A. Yacout, T. Kim, J. Nucl. Mater. 441 (2013) 520.
- [3] E. Losada, J. Garcés, J. Nucl. Mater. 466 (2015) 638.
- [4] A. Landa, P. Söderlind, B. Grabowski, P.E.A. Turchi, A.V. Ruban, L. Vitos, Actinides and nuclear energy materials, MRS Proc. 1444 (2012) 67–78 also available as LLNL-CONF-552336 at, <https://e-reports-ext.llnl.gov/pdf/608332.pdf>.
- [5] A. Landa, P. Söderlind, P. Turchi, J. Nucl. Mater. 414 (2011) 132.
- [6] X. Wang, X. Cheng, Y. Zhang, R. Li, W. Xing, P. Zhang, X.-Q. Chen, Phys. Chem. Chem. Phys. 16 (2014) 26974.
- [7] B.-Q. Liu, X.-X. Duan, G.-A. Sun, J.-W. Yang, T. Gao, Phys. Chem. Chem. Phys. 17 (2015) 4089.
- [8] P. Blaha, K. Schwarz, G.K.H. Madsen, D. Kvasnicka, J. Luitz, WIEN2k: an Augmented Plane Wave + Local Orbitals Program for Calculating Crystal Properties, 2013. User's Guide, WIEN2k 13.1 (Release 25.06.2013).
- [9] P. Söderlind, O. Eriksson, B. Johansson, J.M. Wills, A.M. Boring, Nature 374 (1995) 524.
- [10] J. Perdew, K. Burke, M. Ernzerhof, Phys. Rev. Lett. 77 (1996) 3865.
- [11] P.E. Blöchl, O. Jepsen, O.K. Andersen, Phys. Rev. B 49 (1994) 16223.
- [12] A. Togo, I. Tanaka, Scr. Mater. 108 (2015) 1.
- [13] A. Kokalj, Computational materials science, in: Proceedings of the Symposium on Software Development for Process and Materials Design, vol. 28, 2003, p. 155.
- [14] J. Garcés, G. Grad, A.F. Guillermet, S. Sferco, J. Alloys Compd. 289 (1999) 1.
- [15] J. Nye, Physical Properties of Crystals: Their Representation by Tensors and Matrices, Oxford science publications (Clarendon Press, 1985, p. 142.
- [16] L. Fast, J.M. Wills, B. Johansson, O. Eriksson, Phys. Rev. B 51 (1995) 17431.
- [17] W. Voigt, Lehrbuch Der Kristallphysik (Teubner, 1928).
- [18] A. Reuss, Z. Angew. Math. Mech. – J. Appl. Math. Mech./Zeitschrift für Angewandte Math. und Mech. 9 (1929) 49.
- [19] R. Hill, Proc. Phys. Soc. Sect. A 65 (1952) 349.
- [20] S. Pugh, Lond. Edinb. Dublin Philosophical Mag. J. Sci. 45 (1954) 823.
- [21] X.-P. Gao, Y.-H. Jiang, Y.-Z. Liu, R. Zhou, J. Feng, Chin. Phys. B 23 (2014) 097704.
- [22] Y.L. Hao, S.J. Li, B.B. Sun, M.L. Sui, R. Yang, Phys. Rev. Lett. 98 (2007) 216405.
- [23] S.I. Ranganathan, M. Ostojia-Starzewski, Phys. Rev. Lett. 101 (2008) 055504.
- [24] D.H. Chung, W.R. Buessem, J. Appl. Phys. 38 (1967) 2010.
- [25] O. International Symposium on Anisotropy in Single-Crystal Refractory Compounds (1967 : Dayton, e. Vahldiek, Fred W, e. Mersol, Stanley A, O. C. United States Air Force Materials Laboratory, Dayton, and G. Branch, Anisotropy in Single-crystal Refractory Compounds : Proceedings of an International Symposium on Anisotropy in Single-crystal Refractory Compounds Held on June 13–15, 1967 in Dayton, Ohio, United States Air Force, 1968 sponsored by the Ceramics and Graphite Branch of the Air Force Materials Laboratory.
- [26] W. Setyawan, S. Curtarolo, Comput. Mater. Sci. 49 (2010) 299.
- [27] T. Berlincourt, J. Phys. Chem. Solids 11 (1959) 12.
- [28] A. Adamska, R. Springell, T. Scott, Thin Solid Films 550 (2014) 319.